J Mater Sci: Mater Med (2007) 18:1563–1577
DOI 10.1007/s10856-007-3030-9

Formulation and characterization of chitosan-based hydrogel films having both temperature and pH sensitivity

Guoming Sun · Xian-Zheng Zhang · Chih-Chang Chu

Received: 28 April 2005 / Accepted: 5 May 2006 / Published online: 5 May 2007

Abstract Chitosan-based hydrogel films having both temperature and pH sensitivity were prepared by blending chitosan with temperature sensitive poly (*N*-isopropylacrylamide) (PNIPAAm) and polyethylene glycol (PEG, Mw 2000). PEG was added to enhance film properties, such as thermal, mechanical and swelling properties. Differential scanning calorimetry (DSC) study indicated that the physically blended films exhibited a lower critical solution temperature (LCST) identical to that of pure PNIPAAm (around 32 °C). FT-IR data indicated that the temperature sensitivity is due to the PNIPAAm component in the film. The thermal analysis showed that chitosan and PNIPAAm were compatible and the blended films are apt to crystallize. The X-ray diffraction study further showed that the blended films had a higher crystallinity level than chitosan or PNIPAAm alone. The newly formed crystalline domains acted as physical crosslinkers and greatly increased the crosslinking level of the blended films, which, in turn, affected the swelling behavior and mechanical property of the blended films. Scanning electron microscopy (SEM) revealed that the blended swollen films exhibited a more porous structure at 37 °C (>LCST) than at room temperature (<LCST), though their swelling ratios were reduced as temperature increased from room temperature to 37 °C because of the dehydration nature of PNIPAAm at temperatures above its LCST. The results demonstrated that physically blended temperature sensitive films could be formulated, which are capable of producing more pores upon heating. The blended films were also found to be pH sensitive due to the fact that chitosan, one of the film components, has many pendant amino groups.

G. Sun · X.-Z. Zhang · C.-C. Chu (✉)
Fiber and Polymer Science Program, Department of Textiles and Apparel & Biomedical Engineering Program, Cornell University, Ithaca, NY 14853-4401, USA
e-mail: cc62@cornell.edu

Introduction

A hydrogel is a three-dimensional (3D) crosslinked network that can swell dramatically in the presence of liquid medium and retains a large amount of liquid while maintaining its structure. Due to the high water content, similar to living human tissues [1], hydrogels have found various applications in the fields of tissue engineering and controlled drug release.

One of the most interesting hydrogels is the smart or intelligent hydrogel [2]. Such hydrogels have the capability of responding to some external stimuli, such as temperature [3–5], pH [4, 5], electric and photo fields [6–8]. Due to their diverse functionalities, intelligent hydrogels have received extensive investigations during the past decades. Among these intelligent hydrogels, temperature sensitive hydrogels are the most studied [9]. Currently, poly(*N*-isopropylacrylamide) (PNIPAAm) is the most well-known temperature-sensitive polymer with a lower critical solution temperature (LCST) at around 32 °C. At a temperature below its LCST, linear PNIPAAm is water-soluble; however, at a LCST temperature or higher, the hydrogen bond interactions between PNIPAAm and water become weak and water would be released. As a result, PNIPAAm would undergo a coil to globule transition and become insoluble [10–14].

Attributed to such a unique characteristic, intelligent hydrogels have been extensively studied as devices for controlled drug delivery. Generally, an ideal controlled

release mechanism for a drug carrier is the zero-order drug release; namely, the release rate is independent of time. However, it is more desirable if drugs could be administered in a temporal manner to match physiological needs [14]. Based on such a concept, some types of smart delivery devices have been developed and are able to display an 'on-off' switch capability upon responding to temporal stimuli. Temperature sensitive hydrogels are one of these developments that have attracted significant attention. As a temperature sensitive drug delivery device, traditional PNIPAAm hydrogels usually shrink upon heating above their LCST, and the hydrogels quickly form a dense, less permeable surface layer [15, 16]. This shrinking process usually gives rise to an initial burst release of impregnated drugs followed by a gradual slow release. The dense skin layer formation during the shrinking process of PNIPAAm hydrogels could retard the complete release of large size biomacromolecules like protein-based drugs. For the purpose of a near complete release of larger size biopolymers, those PNIPAAm-based hydrogels that could form or retain pores and release channels after structural shrinkage would be more desirable [17, 18].

Most of the intelligent polymers studied respond to only one type of stimuli. However, for some applications, combined response to several factors, such as temperature and pH, may be desirable [19]. The physiological study reveals that the stomach has a low pH (<3), which is quite different from the neutral intestine. Such pH difference has drawn more attention to pH sensitive hydrogels. From the structure point of view, all pH sensitive hydrogels have either acidic or basic groups, which can respond to pH stimulus by gaining or losing protons.

Although there are various types of hydrogels, only two crosslinking methods have been developed to prepare hydrogels: chemical or physical crosslinking. Chemically crosslinked hydrogels are the most widely studied because of their easy manipulation by controlling the crosslinking agents, initiator concentration, precursor ratio and concentration. However, most crosslinking agents and initiators are toxic, and their residues have to be removed or extracted after preparation [20]. Furthermore, many chemically formed hydrogels, such as PNIPAAm-based, are not biodegradable. Degradation has to be taken into consideration when designing biomedical hydrogels. Physically crosslinked hydrogels may help overcome these disadvantages, and thus they have received more research attention recently [21–24]. During the preparation of physically crosslinked hydrogels, no crosslinking agents or initiators are used, and crosslinks are usually provided through hydrogen or ionic bonds, van der Waal's interactions, crystal formation and/or physical entanglements [25–27]. Physically crosslinked systems, however, are not as strong and stable as covalent bonded systems and can disintegrate much easier and faster.

In this study, we incorporated the temperature sensitive polymer, PNIPAAm, into a biodegradable, biocompatible and nontoxic polysaccharide, i.e., chitosan, to form physically blended films that would have both temperature and pH sensitivity. Chitosan, namely, the *N*-deacetylation of chitin, is the second most abundant polysaccharide on earth. Due to its intriguing biological properties, chitosan has long been known and used in pharmaceutical [28] and biomedical [29] applications. Because of its unusual bioactivity, the formulation of chitosan with drugs has dual therapeutic effects, which make chitosan to be a novel candidate as drug carriers. Poly(ethylene glycol) (PEG) was chosen to be incorporated into the chitosan/PNIPAAm blending system for several reasons. First, PEG could improve flexibility and ductility of the blended films because both chitosan and PNIPAAm are rigid linear polymers, and their blended films were even more brittle. PEG has many attractive properties, such as a wide range of molecular weights, excellent solubility in an aqueous medium, low toxicity and chain flexibility. PEG is non-biodegradable but readily excreted from the body via kidneys and forms nontoxic metabolites. In addition, the incorporation of PEG was expected to improve the biocompatibility of this new blended film according to Zhang et al. report [30]. These blended films were characterized by FT-IR, differential scanning calorimetry (DSC), X-ray diffraction, mechanical strength, swelling ratio, pH sensitivity and morphology.

Experimental procedures

Materials

Chitosan (Mw 400,000) was purchased from Fluka Chemie AG (Buchs, Switzerland). Acetic acid was purchased from EM Science Industries (Gibbstown, NJ). PEG (Mw 2000), benzoyl peroxide (BPO) and *N*-isopropylacrylamide (NIPAAm) were purchased from Aldrich Chemical Company (Milwaukee, WI); NIPAAm was further purified with benzene/*n*-hexane by recrystallization. The buffer solution of pH 3 was purchased from Fisher Scientific (Fair Lawn, NJ), and other buffer solutions of pH 4.0, 5.0, 7.0, 10.0 were purchased from GFS chemicals (Powell, OH).

Film preparation

PNIPAAm was prepared by free radical polymerization in methanol according to our previous method [31]. Briefly, the polymerization of NIPAAm (5.65 g, 50 mmol in methanol) in a 150 mL flask under dry nitrogen atmosphere was initiated by BPO (0.242 g, 2.0 mol% based on

NIPAAm) at 70 °C for 24 h. After polymerization, the resulting product was precipitated in excess diethyl ether. The product was further purified by dissolution in acetone and reprecipitation in diethyl ether 3 times. The purified product was dried in vacuum at room temperature for 24 h. PNIPAAm of molecular weight 33,000 was obtained.

All film samples were prepared by a traditional dissolution/evaporation method. In brief, 0.6 g of chitosan/PEG/PNIPAAm blends of different composition ratios (see Table 1) were dissolved in 70 mL acetic acid solution (2% v/v). After shaking for 2 days, the solution was then filtered through a glass Buchner funnel to remove the undissolved materials. The solution was cast onto Petri dishes (100×10 mm^2) and dried for 2 days in a fume hood. The resulting films were further dried in vacuum for 2 days at room temperature. A series of blended films of thickness from 0.5 mm to 1.0 mm were prepared and the films obtained were designated as fresh films.

Three types of physically blended chitosan/PEG/PNIPAAm films were prepared from chitosan, PNIPAAm and PEG components, and their feed compositions and sample ID are summarized in Table 1. The chitosan/PNIPAAm films (CGNI) were first prepared; to modify their property, PEG was then introduced into CGNI to fabricate chitosan/PEG/PNIPAAm films. In this study, two series of chitosan/PEG/PNIPAAm films were prepared: one with a constant PNIPAAm composition (CGNII) and the other with a constant PEG composition (CGNIII). The chitosan/PEG/PNIPAAm films were labeled as CGN. The composition of the film is expressed as CGN#/#/#. For example, the chitosan/PEG/PNIPAAm film of a composition of 60% chitosan, 20% PEG and 20% PNIPAAm is labeled as CGN60/20/20. It is worth noting that neither PEG nor PNIPAAm alone can form a film, thus no pure PEG or PNIPAAm films were prepared in this study.

FT-IR characterization

To study the composition changes before and after swollen as well as the possible interactions among components, both fresh and freeze-dried swollen films were characterized by FT-IR (Nicolet Magna 560, Madison, WI). The freeze-dried films were obtained by immersing fresh films in distilled water at both room temperature and 37 °C for 3 h; the swollen films were quickly frozen in liquid nitrogen and further freeze-dried in a Virtis Freeze Drier (Gardiner, NY) under vacuum at –50 °C for 3 days until the samples became completely dry prior to characterization. Both the fresh and freeze-dried film samples were directly placed on the horizontal Attenuated Total Reflectance (ATR) attachment of a Nicolet Magna 560 FT-IR for recording IR spectra without the use of KBr powder. The pure chitosan film was characterized by the ATR method as well. Pure PEG or PNIPAAm powders, however, were mixed with KBr powder (1/10, w/w) and compressed into pellets for normal FT-IR measurement (without ATR).

X-ray diffraction

To study the crystalline characteristics of the blended films, an X-ray diffractometer (WAXD, Scintag, Cuttertino, CA) was employed to obtain the wide X-ray diffraction patterns. In this study, the WAXD patterns were obtained under the condition of 45 kV and 40 mA with a continuous scan mode at the speed of 2.5°/min from 5° to 35°. The pure chitosan film and the blended films were horizontally mounted on the holder, while the pure PEG and PNIPAAm powders were placed in a tray and then mounted onto the holder.

DSC measurement

Glass transition and crystallization temperatures

The thermal property of films were measured by DSC (2920 modulated DSC, TA instruments, CA). The fresh films were cut into small pieces, and about 10 mg of such film samples were placed inside an aluminum sample pan. An empty sample pan was used as a reference. The thermal analysis was performed from 30 °C to 300 °C at the heating rate of 10 °C/min under dry nitrogen atmosphere with a flow rate of 25 mL/min. Pure chitosan and PNIPAAm were also tested under the same condition. TA universal analysis software was used for data analysis. The inflection of the DSC curve was used to determine T_g by TA universal analysis software, and crystallization peak was referred as the crystallization transition temperature (T_c).

Table 1 Feed compositions of the chitosan/PEG/PNIPAAm hydrogel films

Film composition	CGN I					CGN II							CGN III						
	A	B	C	D	E	A	B	C	D	E	F	G	A	B	C	D	E	F	G
Chitosan (g)	0.60	0.51	0.45	0.39	0.33	0.51	0.48	0.45	0.42	0.39	0.36	0.33	0.48	0.45	0.42	0.39	0.36	0.33	0.30
PEG (g)	0.00	0.00	0.00	0.00	0.00	0.00	0.03	0.06	0.09	0.12	0.15	0.18	0.12	0.12	0.12	0.12	0.12	0.12	0.12
PNIPAA (g)	0.00	0.09	0.15	0.21	0.27	0.09	0.09	0.09	0.09	0.09	0.09	0.09	0.00	0.03	0.06	0.09	0.12	0.15	0.18

LCST determination

The LCST of the swollen films was determined by DSC. The fresh films were immersed in distilled water at room temperature for 3 h before testing. About 10 mg swollen fresh films were placed inside a hermetic aluminum pan, and sealed tightly by a hermitic aluminum lid. An empty sealed aluminum pan was used as a reference. The samples were heated from 0 °C to 50 °C at the rate of 3 °C/min under dry nitrogen atmosphere with a flow rate of 25 mL/min. TA universal analysis software was used for the data analysis. The onset point of the endothermic change of the DSC curve was referred to LCST.

Swelling tests

The swelling properties of all films were gravimetrically studied. A known weight of film sample was immersed in distilled water at both room temperature (25 °C) and 37 °C. The swollen films were removed at predetermined intervals and weighed after wiping off the excess water on the film surface with a wet filter paper. The swelling ratio is defined and calculated as below:

$$\text{Swelling ratio}(\%) = [(W_t - W_d)/W_d] \times 100\%$$

where W_t is the weight of swollen film at time t, and W_d is the weight of dry film at time 0.

Morphological study

The surface morphological changes of the swollen films at both room temperature and 37 °C were studied using a scanning electron microscope (XL Series-30; Philips, Hillsboro, OR). Small pieces of films (10×10 mm^2) were cut and immersed in distilled water for 3 h at both room temperature and 37 °C. The swollen films were then freeze-dried for 3 days prior to SEM observation. The specimens were mounted onto aluminum stubs with double-sided carbon tape and sputter-coated with gold for 60 s (JFC-1200 Fine Coater, Japan).

Mechanical properties

The tensile property of all films was measured by an Instron (model 1122, Instron Corporation) at the condition of 22 °C and 65% relative humidity. The specimens were cut into 10 mm wide, 70 mm long stripes. The width and thickness were measured three times at three different positions, respectively, for each sample, and the averages were then obtained. The gauge length of the Instron was set to 40 mm and the crosshead speed was 50 mm/min. The stress, strain, toughness and modulus were used to evaluate the mechanical property of the films.

pH sensitivity

The pH sensitivity of the blended films was investigated by studying its swelling behavior in buffer solutions of different pH (3.0, 4.0, 5.0, 7.0, and 10.0). In this study, the CGN60/20/20 film was chosen as the model sample because the chitosan composition of this blended film was between the minimum and maximum ratios, which might better represent the pH sensitive property of the blended films. All film samples were immersed in a buffer solution of predetermined pH at room temperature. At the end of predetermined intervals, the swollen films were removed, wiped and weighed, and their swelling ratios were calculated the same way as defined in the previous swelling tests section.

Results and discussion

FT-IR analysis

FT-IR was used to determine any chemical changes in the blended film composition before and after swelling as well as any possible interactions among film components. Figure 1 shows the spectra of individual polymer components and one of their physically blended swollen films at the composition of CGN70/20/10. The IR peaks 1 and 2 (1,103 cm^{-1}) of spectrum A (PEG) and D (CGN70/20/10) are the typical position for the C–O stretching of PEG, which appeared only in PEG (spectrum A) and the fresh

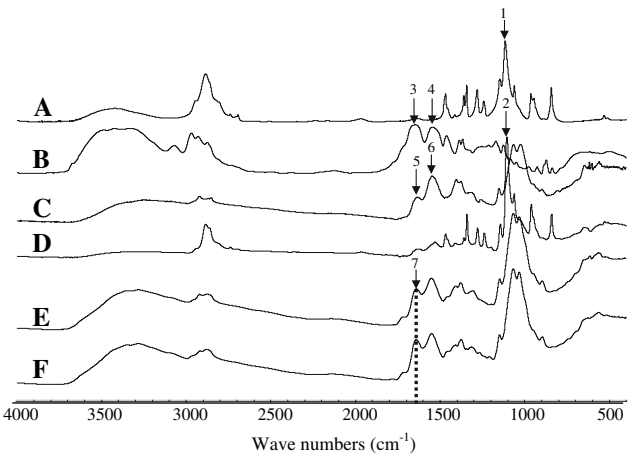

Fig. 1 FT-IR spectra of chitosan/PEG/PNIPAAm hydrogel films (**A**) PEG; (**B**) PNIPAAm; (**C**) chitosan; (**D**) fresh CGN70/20/10 (**E**) Freeze fried CGN70/20/10 film swollen at room temperature; (**F**) Freeze dried CGN70/20/10 hydrogel film at 37 °C (1&2: ~1,103 cm^{-1}, 3: ~1,650 cm^{-1}; 4: ~1,543 cm^{-1}; 5: ~1,630 cm^{-1}; 6: ~1,547 cm^{-1}; 7: ~1,642 cm^{-1})

film (spectrum D). However, this peak almost could not be detected in those films after swelling in both room temperature and 37 °C (spectra E and F). These results suggest that most PEG was leached out from the blended films during swelling. Similar findings was reported by Zhang et al. [10] in their study of PEG-impregnated PNIPAAm hydrogels in which PEG was used as a pore-forming agent and leached out after swelling. The FT-IR peaks at 1,650 and 1,543 cm^{-1} were attributed to amide I and amide II of PNIPAAm. The peak of 1,630 cm^{-1} was from amide I of chitosan, and 1,547 cm^{-1} from amide II and C–N stretching of amine group of chitosan.

The FT-IR spectra of the swollen films also revealed the interaction between PNIPAAm and chitosan. After swelling and freeze-drying, spectra E and F showed only one shifted amide I peak (peak 7 at 1,642 cm^{-1}). This result suggests that PNIPAAm and chitosan had some interactions with each other in the blending, which led to amide I peak shift to the location between pure chitosan (peak 5) and pure PNIPAAm (peak 3). These FT-IR data suggest that PNIPAAm still remained in the blended film and was miscible with chitosan.

The FT-IR spectra of freeze-dried swollen films of different compositions at both room temperature and 37 °C are shown in Figs. 2 and 3, respectively. The FT-IR spectra indicate that, after swelling at both room temperature and 37 °C, PNIPAAm remained in all these freeze-dried blended films. Furthermore, based on the absorbance intensity ratio of amide I/amide II (0.844 and 0.908), we observed that more PNIPAAm remained in the blended films after swelling at 37 °C (0.908) than the same film swelling at room temperature (0.844). This difference in PNIPAAm contents remaining in the blended films after swelling at different temperatures could be attributed to the thermal property of PNIPAAm. It is well known that at temperatures above its LCST, PNIPAAm will experience a coil-to-globule transition, which makes PNIPAAm more hydrophobic and becomes hard to dissolve, i.e., retaining more PNIPAAm within blended films. However, at room temperature, PNIPAAm is water-soluble. Thus, more PNIPAAm can be kept in the blended film at 37 °C swelling than at room temperature one.

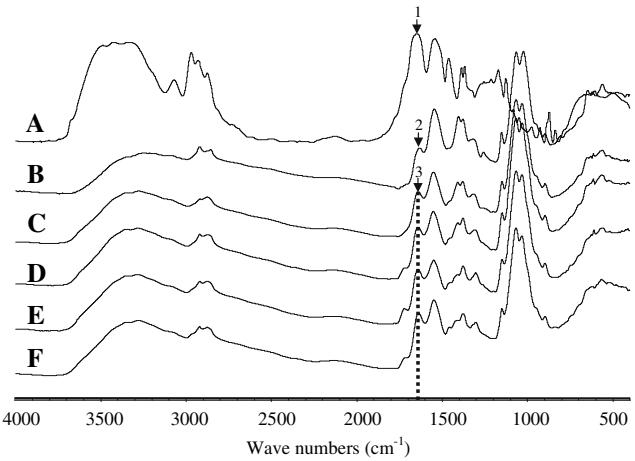

Fig. 2 FT-IR spectra of freeze-dried chitosan/PEG/PNIPAAm hydrogel films swollen at room temperature (**A**) PNIPAAm; (**B**) chitosan; (**C**) CGN75/20/5; (**D**) CGN70/20/10; (**E**) CGN60/20/20; (**F**) CGN50/20/30 (1: ~1,650 cm^{-1}; 2: ~1,630 cm^{-1}; 3: ~1,642 cm^{-1})

X-ray diffraction

The X-ray data of PEG, chitosan, PNIPAAm and their blends are shown in Fig. 4. PEG (spectrum A) exhibited very strong peaks at $2\theta = 19.1°$ and 23.3°, which were assigned to (120) and (–212), respectively [32]. PNIPAAm (spectrum B) showed two diffraction peaks at $2\theta = 7.5°$ and 19.4°, which are also in agreement with Kim's results [33]. Chitosan (spectrum C) showed two peaks at $2\theta = 13.4°$ and 19.5°, and these peaks were assigned to a mixture of (001) and (100), (101) and (002), respectively [33, 34]. The crystallization of chitosan is actually quite complicated. It has been reported that the crystalline structure of chitosan depends on the degree of deacetylation [35, 36] and preparation procedures [37].

The X-ray diffraction data of CGN80/20/0(spectrum D) in Fig. 4 suggest that the blending of two crystallizable components (PEG and chitosan) would not automatically lead to crystallizable blends; and retardation of crystallization in the chitosan/PEG blend could actually occur (D in Fig. 4). It is reported that the reason that chitosan is stable in a neutral pH condition is because the amine and hydroxyl groups on glucosamine units can form inter- and intra-molecular hydrogen bonds to facilitate and stabilize chitosan crystalline structure [38]. The incorporation of PEG, which acted as a plasticizer, into chitosan could disrupt the formation of hydrogen bonds between amino and hydroxyl groups in chitosan, i.e., retarding chitosan molecules to organize into ordered packing and hence becoming amorphous chitosan. On the other hand, the interaction between PEG and the relatively stiffer chitosan macromolecules could also retard the mobility of PEG, i.e., making PEG macromolecules difficult to reorganize into orderly and crystallizable position [39]. As a result, PEG could not form crystals in this film (D in Fig. 4).

In the blend of chitosan and PNIPAAm (CGN65/0/35, E in Fig. 4), the blend film showed a reduced crystallinity level than pure PNIPAAm (B in Fig. 4) and chitosan (C in Fig. 4). This reduction in crystallinity level is believed to be attributed to the intermolecular interactions between PNIPAAm and chitosan. Such intermolecular interactions were evident in the FT-IR spectra (e.g., E and F spectra in Fig. 1) in which chitosan and PNIPAAm macromolecules

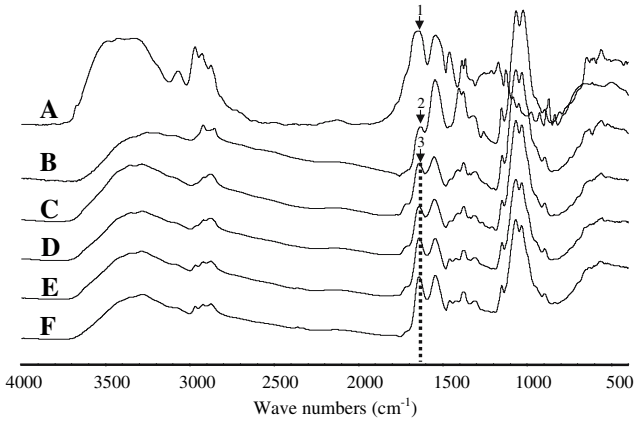

Fig. 3 FT-IR spectra of freeze-dried chitosan/PEG/PNIPAAm hydrogel films swollen at 37 °C (**A**) PNIPAAm; (**B**) chitosan; (**C**) CGN75/20/5; (**D**) CGN70/20/10; (**E**) CGN60/20/20; (**F**) CGN50/20/30 (1: ~1,650 cm^{-1}; 2: ~1,630 cm^{-1}; 3: ~1,642 cm^{-1})

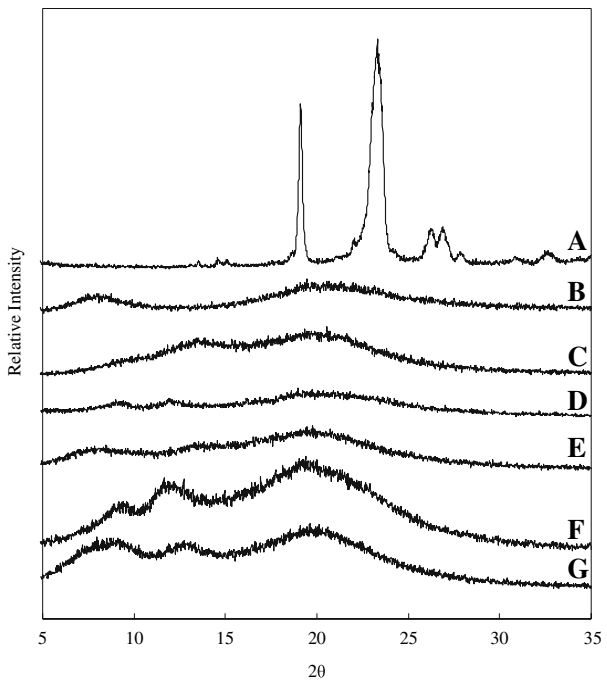

Fig. 4 Wide angle X-ray spectra of fresh chitosan/PEG/PNIPAAm hydrogel films (**A**) PEG; (**B**) PNIPAAm; (**C**) chitosan; (**D**) CGN80/20/0, (**E**) CGN65/0/35; (**F**) CGN70/20/10; (**G**) CGN60/20/20

could interact with each other through their amide groups. This interaction between chitosan and PNIPAAm would disrupt the inherent hydrogen bonding formation among chitosan molecules and among PNIPAAm molecules. Such a disruption would reduce the crystallization capability of the blended chitosan/PNIPAAm film. Besides, the strong intermolecular interaction between chitosan and PNIPAAm would also reduce the chain flexibility and mobility of these macromolecules, which could also retard the regular and order arrangement of PNIPAAm and chitosan macromolecules. Therefore, due to the disruption of the inherent H-bond capability of chitosan and PNIPAAm and the establishment of strong intermolecular interaction between chitosan and PNIPAAm, the chitosan/PNIPAAm blended film showed a reduced crystallinity level.

Surprisingly, the blends of chitosan, PEG and PNIPAAm (F and G in Fig. 4) show a higher level of crystallinity than pure PNIPAAm (B in Fig. 4), chitosan (C in Fig. 4), though a lower crystallinity level than pure PEG (A in Fig. 4). As mentioned before, the incorporation of PEG could reduce the crystallinity of pure chitosan (D in Fig. 4); however, the crystallinity level of the blends of chitosan, PEG and PNIPAAm (F and G in Fig. 4) was significantly higher after PEG was introduced into the chitosan/PNIPAAm blends. It is believed that a blend of chitosan and PNIPAAm has some strong intermolecular forces, including the hydrogen bond between chitosan and PNIPAAm, which could reduce the chain mobility of both chitosan and PNIPAAm, i.e., a reduction in their ability to crystallize. The addition of PEG into the chitosan/PNIPAAm blend, however, would not only weaken the interaction between chitosan and PNIPAAm, but also could generate additional space between chitosan and PNIPAAm to facilitate rearrangement of chain segments into ordered position for crystallization. At the same time, the interaction between PEG and chitosan and PNIPAAm macromolecules could retard the mobility of PEG, i.e., making PEG macromolecules difficult to reorganize into ordered and crystallizable position, i.e., no PEG crystallinity was detected in the blends of chitosan, PNIPAAm and PEG.

Thermal analysis

The thermal properties of the blended films were measured by DSC and their results are shown in Fig. 5. Chitosan (Curve F) has no clear glass transition temperature (T_g) [40] though many researchers had tried to determine it and a wide range of T_g from 161 °C to 203 °C has been reported [41–43]. Although chitosan had some crystalline regions as shown in Fig. 4 (curve C), its crystalline melting temperature (T_m) could not be found because strong inter- and/or intra-molecular hydrogen bonds lead to rigid-rod polymer backbone [32], which, like cellulose, would degrade before reaching its melting point. PNIPAAm showed a T_g at around 141 °C (curve E). The other blended films showed a lower T_g than pure PNIPAA, ranging from 115 °C to 120 °C.

Traditionally, the glass transition temperature has been used to study interaction and miscibility of polymer blends. If the blend would have one medially shifted T_g, the blend would have a good miscibility among components. If multiple T_g would be found in a blend, it would suggest

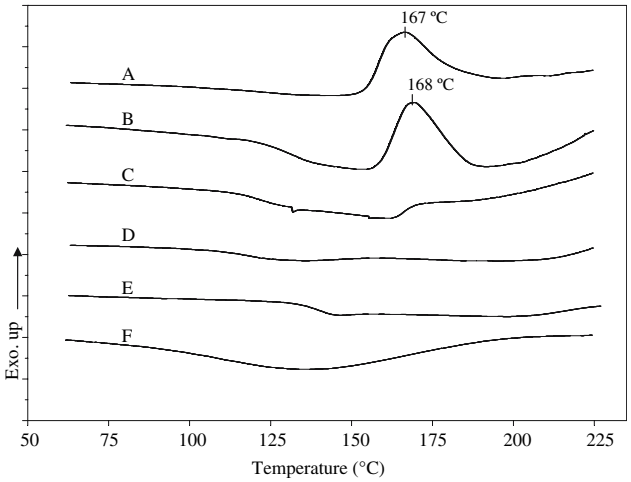

Fig. 5 DSC thermograms of fresh Chitosan/PEG/PNIPAAm hydrogel films (**A**) CGN70/20/10; (**B**) CGN60/20/20; (**C**) CGN80/20/0; (**D**) CGN65/0/35; (**E**) PNIPAAm; (**F**) chitosan

poor miscibility. In this study, the chitosan/PNIPAAm blend had only one shifted glass temperature transition when compared to pure PNIPAAm, an indication that PNIPAAm and chitosan were compatible, though chitosan did not have a meaningful T_g. The FT-IR spectra (e.g., E and F spectra in Fig. 1) also indicated that chitosan and PNIPAAm could interact with each other through their amide groups, which would facilitate their miscibility. The blend of chitosan/PEG (C in Fig. 5) showed a slightly different DSC trace from chitosan itself.

The two chitosan/PEG/PNIPAAm blended films, i.e., CGN70/20/10 (A in Fig. 5) and CGN60/20/20 (B in Fig. 5), showed quite different DSC thermograms from other blends and pure controls as these two blends had distinctive exothermal peaks at 167–168 °C. These exothermal peaks were attributed to crystallization, during which heat was released after the macromolecules became closely packed. This result demonstrates that the blend of chitosan/PEG/PNIPAAm has the capability to crystallize, which was also supported by the X-ray results given above (F and G in Fig. 4). The role of PEG in the PEG/chitosan/PNIPAAm blends is to act as a plasticizer, which could not only weaken the interactions between chitosan and PNIPAAm but also could generate additional space for chitosan and PNIPAAm to rearrange into ordered position. Therefore, upon heating, both chitosan and PNIPAAm gained enough energy to move to their new positions to form thermally stable crystals, which can be seen from the twin peaks in X-ray diffraction data (F and G in Fig. 4) as well as the distinctive crystallization peaks (A and B in Fig. 5).

The ability for blended components to crystallize in a physically blend system is important in terms of miscibility and stability. During crystallization, system entropy will decrease since molecules become more closely and orderly packed due to the polar interactions, i.e., mainly hydrogen bond interactions between amine groups of chitosan and the amide groups of PNIPAAm in this blending. The lower energy state of a blending system would make such a blend system thermodynamically more stable. The induced crystals could also serve as physical crosslinkers to improve the stability of the system.

LCST behavior

The temperature sensitivity of the blended films was confirmed by the presence of the LCST. Both Tables 2 and 3 show that all blended films had a LCST near 32 °C, though there's a slight but consistent increase in the LCST with an increase in PEG (Table 2) or PNIPAAm content (Table 3). For example, in Table 2, the LCST of the blended films increased from 31.5 °C to 32.9 °C when the PEG content increased from 0% to 30%; while in Table 3, the LCST of the blended films increased from 30.7 °C to 32.3 °C when the PNIPAAm content increased from 0% to 30%. However, no LCST was detected in the CGN80/20/0 film, which confirms that the LCST was from PNIPAAm macromolecules.

Generally, the temperature sensitivity of PNIPAAm is usually attributed to the rapid alternation between hydrophilicity and hydrophobicity upon heating. At temperatures below LCST, water molecules adjacent to the pendant amide groups of PNIPAAm form hydrogen bonds with these groups and assume a stable pentagonal (icelike) structure. However, at higher temperatures (>LCST), the extra thermal energy provided can lead to thermal dissociation of the hydrogen bonds between water and the pendant amide groups of PNIPAAm macromolecules; such breakage of H-bonds would facilitate the formation of hydrophobic interaction arising from the intrinsic hydrophobic affinity among the pendant isopropyl groups of PNIPAAm polymer chains and prompts PNIPAAm to collapse and behave like a hydrophobic polymer. Hydrophobic interactions among isopropyl pendant groups increase with time and the PNIPAAm macromolecules start to aggregate and phase separation occurs. As a result, the hydrogel volume collapses at the temperature above its LCST, and the hydrogels appear to be hydrophobic. The water molecules entrapped within the hydrogels could then be freed due to the broken hydrogen bonds. Therefore, the main mechanism for the phase separation of the temperature sensitive polymers involves the changes of the hydration-dehydration behavior in these systems.

The temperature sensitivity of PNIPAAm may also be described from the thermodynamic point of view. At temperatures < LCST, the enthalpy would dominate during the formation of H-bonds at the expense of unfavorable

Table 2 LCST of chitosan/PEG/PNIPAAm hydrogel films as a function of PEG content

Film	A	B	C	D	E	F	G
Composition	80/0/15	80/5/15	75/10/15	70/15/15	65/20/15	60/25/15	55/30/15
LCST (°C)	31.5	31.7	31.8	31. 9	32.2	32.8	32. 9

Table 3 LCST of chitosan/PEG/PNIPAAm hydrogel films as a function of PNIPAAm content

Film	A′	B′	C′	D′	E′	F′	G′
Composition	80/20/0	75/20/5	70/20/10	65/20/15	60/20/20	55/20/25	50/20/30
LCST (°C)	–	30.7	31.6	32.1	32.2	32.8	32.3

entropy change (reduction in entropy). However, at temperatures >LCST, the entropy would dominate due to the thermal dissociation of H-bonds and the formation of free water.

Because PNIPAAm moiety was solely responsible for the thermo-responsive property in the blended films, it is understandable that the LCST of the blended films is similar to the pure PNIPAAm, i.e., ~32 °C, and the chitosan and PEG components had little impact on the LCST of the blend films. Since the temperature sensitivity of PNIPAAm involves the interaction between amide group and water molecules, the LCST change of the blended films could be attributed to the interaction between PNIPAAm with other molecules in the blended films.

In Table 2, the blend film without PEG (sample A) had the lowest LCST, i.e., needed the least amount of thermal energy to break H-bonds between water and PNIPAAm. This is because, in the absence of PEG, PNIPAAm and chitosan could exert strong intermolecular action through their amide groups as evidenced by the FT-IR data (e.g., E and F spectra in Fig. 1). This strong intermolecular interaction would leave less room for the interaction between amide groups of PNIPAAm and water molecules, and hence less heat would be needed to break down hydrogen bonds, i.e., a lower LCST as observed. The introduction of PEG would weaken the interactions between PNIPAAm and chitosan, which leave PNIPAAm more opportunity to interact with water molecules. As a result, more heat would be required to break the hydrogen bonds; therefore the LCST of the blended films increased with an increase in PEG content. In addition, the PEG-incorporated chitosan/PNIPAAm films would be more hydrophilic, and such an increase in hydrophilicity in a PNIPAAm system is well-known to increase LCST.

The blended film without PNIPAAm (sample A in Table 3) showed no LCST until PNIPAAm was introduced. As more PNIPAAm introduced, more amide groups would interact with water, thus more heat would be needed to break the hydrogen bonds between amide groups and water molecules, i.e., increasing the LCST with an increasing PNIPAAm content in the blended films.

Swelling tests

Figure 6 shows that, at room temperature, the chitosan/PNIPAAm films could swell more and faster with the addition of PNIPAAm into chitosan. All PNIPAAm incorporated chitosan/PNIPAAm films had a higher swelling ratio than pure chitosan film CGN100/0/0 (curve A). For an instance, within 50 min, the swelling ratio of CGN65/0/35 film (curve E) reached up to twice the swelling ratio of pure chitosan film CGN100/0/0 (curve A). Some of these blended films even disintegrated after 90 min due to their high swelling.

The inclusion of PEG into the blends of chitosan/PNIPAAm, however, significantly reduced the swelling of chitosan/PNIPAAm films as shown in Fig. 7, and the swelling of the blended films decreased significantly with an increase in PEG content. Without PEG, CGN85/0/15

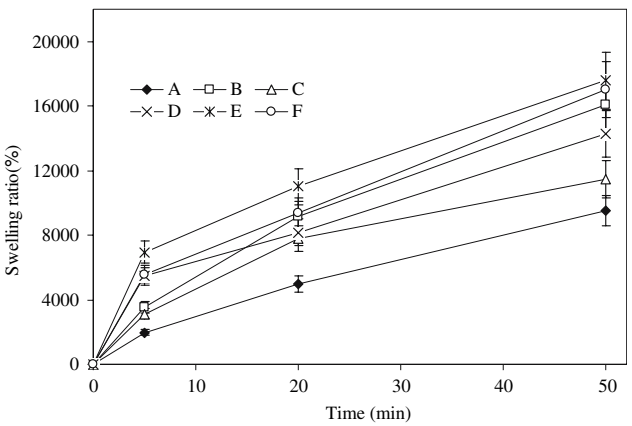

Fig. 6 Effect of PNIPAAm content on the swelling kinetics of chitosan/PEG/PNIPAAm hydrogel films at room temperature. PEG content retained at 0% by weight. (**A**) CGN100/0/0; (**B**) CGN95/0/5; (**C**) CGN85/0/15; (**D**) CGN75/0/25; (**E**) CGN65/0/35; (**F**) CGN55/0/45

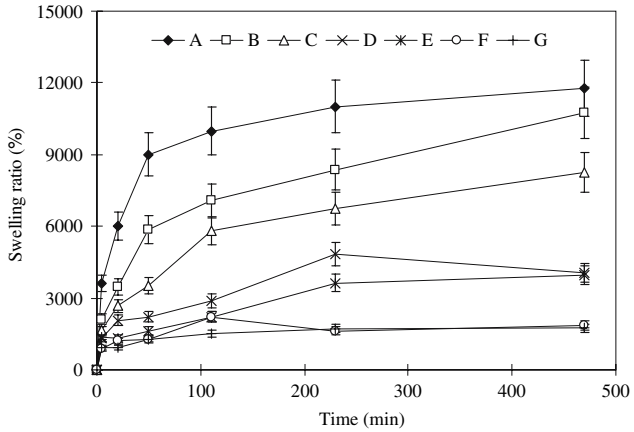

Fig. 7 Effect of PEG content on the swelling kinetics of chitosan/PEG/PNIPAAm hydrogel films at room temperature. PNIPAAm content retained at 15% by weight. (**A**) CGN85/0/15; (**B**) CGN80/5/15; (**C**) CGN75/10/15; (**D**) CGN70/15/15; (**E**) CGN65/20/15; (**F**) CGN60/25/15; (**G**) CGN55/30/15

film (curve A in Fig. 7) swelled to 120 times of its original weight, while CGN60/25/15 (curve F in Fig. 7) only reached 15 times of its original weight in about 7 h. It seems that PEG had no more effect on swelling after its content increased to 25%. When the PEG content remained constant, the swelling ratio of chitosan/PEG/PNIPAAm films decreased with an increase in PNIPAAm content as shown in Fig. 8. Obviously, without PNIPAAm, CGN80/20/0 film (curve A in Fig. 8) swelled very fast and the swelling ratio attained 200 times of its original weight within 50 min; and it even dissociated after 90 min. The swelling ratio of the chitosan/PEG/PNIPAAm films, however, was reduced significantly when PNIPAAm was initially introduced (B in Fig. 8) and the magnitude of

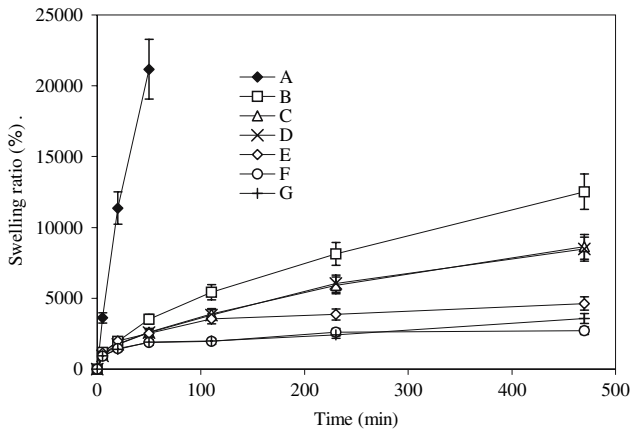

Fig. 8 Effect of PNIPAAm content on the swelling kinetics of chitosan/PEG/PNIPAAm hydrogel films at room temperature. PEG content retained at 20% by weight. (**A**) CGN80/20/0; (**B**) CGN75/20/5; (**C**) CGN70/20/10; (**D**) CGN65/20/15; (**E**) CGN60/20/20; (**F**) CGN55/20/25; (**G**) CGN50/20/30

reduction increased with an increase in PNIPAAm content in the films. This PNIPAAm effect became insignificant when the PNIPAAm content reached beyond 20% by weight (curves F and G of Fig. 8). It is possible that a portion of the reduction in swelling ratio of PEG-containing chitosan/PNIPAAm films might arise from the extraction of PEG from the films as shown in FT-IR data (Fig. 1). However, such PEG extract effect would be minimal when comparing with the thousands % gain in water weight during swelling.

Chitosan is a well-known hydrophilic polymer with outstanding film/gel forming capability. A pure chitosan film (A in Fig. 6) is able to imbibe a lot of water and swells quickly before it disintegrates. However, the data in Fig. 6 show that the PNIPAAm incorporated chitosan/PNIPAAm films became even more water absorbent at room temperature than pure chitosan. This could be attributed to the crystallinity change as well as the disruption of inter/intra-molecular interaction of chitosan by PNIPAAm. As shown in Fig. 4, chitosan/PNIPAAm blends (curve E) had a reduced level of crystallinity when compared to pure chitosan (Curve C) or PNIPAAm (Curve B). This reduction in crystallinity would facilitate more water diffusion into the chitosan/PNIPAAm blends. In addition, PNIPAAm could also weaken the inter/intra-molecular interaction among chitosan molecules, which may even facilitate the diffusion of water. Thus, the chitosan/PNIPAAm films were able to absorb more water or became more water absorbent than pure chitosan film.

The incorporation of PEG reduced the swelling property of chitosan/PNIPAAm films as shown in Fig. 7. Because of its hydrophilicity and chain flexibility, we expected the addition of PEG into the chitosan/PNIPAAm films should increase water absorption. The data in Fig. 7, however, show the opposite of what we expected. An introduction of PEG into the chitosan/PNIPAAm system indeed reduced the swelling ratio from the chitosan/PNIPAAm film, and the swelling ratio decreased as the PEG content increased. Similar findings were also reported in other systems. For example, Bajpai et al. [44] found that the physical impregnation of PEG into HEMA/acrylamide hydrogel reduced the swelling ratio of the hydrogel. Bajpai et al. believed when the PEG content reached to a certain level, the gel network density might become so high that mesh sizes of free volumes available between the network chains reduced and this slowed down the diffusion of water molecules into the gel, i.e., a reduced swelling of the hydrogel. The authors did not give a reason why the mesh size was reduced due to the addition of PEG. For our experiment, the addition of PEG to chitosan/PNIPAAm films was found to increase the crystallinity of the blended films (curves F and G in Fig. 4). The crystalline regions act as crosslinkers to limit the expansion of the network upon

swelling, i.e., impeding the degree of swelling. Furthermore, water molecules also have difficulty to diffuse into crystalline domains. Therefore, the improved crystallinity level upon PEG incorporation into the chitosan/PNIPAAm blend films was the main reason for the observed reduced swelling ratio in chitosan/PEG/PNIPAAm system.

Unlike the chitosan/PNIPAAm films (Fig. 6), the swelling of the blended chitosan/PEG/PNIPAAm films (at a constant PEG content) was reduced with the addition of PNIPAAm (Fig. 8). As discussed above, this reduction in the swelling ratio due to the incorporation of PNIPAAm component is mostly caused by the formation of new crystalline domains in the blended films (spectrum F and G in Fig. 4). Besides the crystallinity contribution toward the reduction in swelling ratio, the strong intermolecular interactions from the entanglement and hydrogen bonds between PNIPAAm and chitosan also reduced swelling. The formation of hydrogen bonds between chitosan and PNIPAAm would reduce the number of the available groups in the network that can form the hydrogen bonds with water molecules, which could also reduce swelling ratio.

We further investigated the swelling behavior of the blended films (CGN70/20/10 and GNG60/20/20) at a temperature above the LCST of PNIPAAm (37 °C), as illustrated in Fig. 9. It was found that the swelling behaviors of the blended films at 37 °C (>LCST) were quite different from those at room temperature (<LCST). both blended films CGN70/20/10 (A in Fig. 9) and CGN60/20/20 (B in Fig. 9) showed a lower but similar swelling profiles at 37 °C than at room temperature. For instance, at 37 °C, both the blended films reached an equilibrium-swelling ratio of 500 within about 6 h, but at room temperature they attained 8–16 times of their swelling ratios at 37 °C; the swelling ratio of film CGN70/20/10 was twice

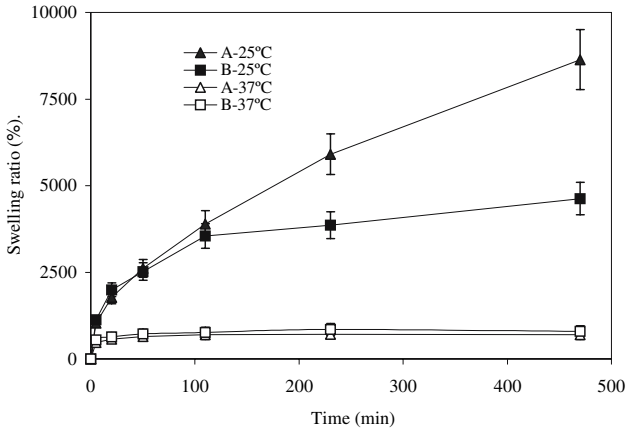

Fig. 9 Effect of temperature (room and 37 °C) on the swelling kinetics of chitosan/PEG/PNIPAAm hydrogel films. (**A**) CGN70/20/10; (**B**) CGN60/20/20

of CGN60/20/20 at room temperature. The difference between CGN70/20/10 and CGN60/20/20 blended films was the PNIPAAm contents and hence their swelling difference was attributed to the same reasons previously described in Fig. 8.

The lower swelling at 37 °C than at room temperature could be attributed to the increased hydrophobicity. It is known that at a temperature below LCST, PNIPAAm moiety in the film becomes hydrophobic, and is difficult to imbibe water. Although chitosan is a hydrophilic polymer and has no temperature sensitivity, the swelling of the blended films were restricted by the hydrophobic nature of the PNIPAAm component at a temperature greater than LCST. As a result, the whole hydrophilic/hydrophobic balance of the blended film shifted to more hydrophobic and a lower swelling ratio was observed at 37 °C.

Morphological study

Figures 10 and 11 show the SEM images of the freeze-dried swollen films at room temperature (25 °C, Fig. 10) and 37 °C (Fig. 11), respectively. The images clearly show two distinctive phenomena: (1) at room temperature, the blended films CGN75/20/5 (A in Fig. 10) and CGN70/20/10 (B in Fig. 10) have a wrinkled, non-fragmented but nonporous surface, while blended films CGN60/20/20 (C in Fig. 10) and CGN50/20/30 (D in Fig. 10) have fragmented and porous appearance on the surface; (2) at 37 °C, all these blended films (except CGN50/20/30, D in Fig. 11) showed significant 3D porous structure (Fig. 11), and the pore size of the blended films was reduced with an increase in PNIPAAm content, while number of pores was greatly increased (A–D in Fig. 11). CGN75/20/5 (A in Fig. 11) has the largest pore size (12.0 ± 2.0 μm), while the pore of CGN 70/20/10 (B in Fig. 11) became smaller (5.0 ± 1.5 μm) as PNIPAAm content increased. The pore size was reduced further with an additional increase in PNIPAAm content in the film. For example, CGN 60/20/20 (C in Fig. 11) had the smallest pore size (1.6 ± 0.7 μm). When the PNIPAAm content reached high enough in the film (30%), no clear 3D round-shaped pores appeared on the surface of CGN50/20/30 (D in Fig. 11), which was virtually identical to the same film at room temperature (D in Fig. 10).

The different morphological appearance (Fig. 10) of the swollen films could be attributed to their different swelling behaviors. As shown in Fig. 8, the swelling ratios of the films CGN75/20/5(B), CGN70/20/10(C), CGN60/20/20(E) and CGN50/20/30(G), (corresponding to film A, B, C, and D in Figs. 10 and 11), reduced with an increase in PNIPAAm content. This swelling reduction, as discussed previously, could be attributed to the newly formed crystalline domains and the strong interactions between chitosan and

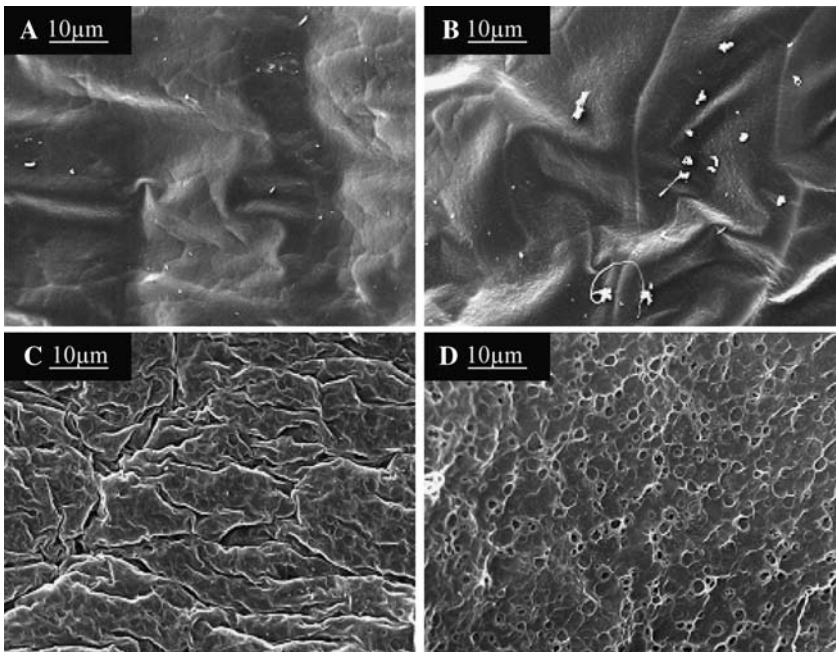

Fig. 10 Effect of PNIPAAm content on the surface morphology of chitosan/PEG/PNIPAAm hydrogel films swollen at room temperature. PEG content retained at 20% by weight. (**A**) CGN75/20/5; (**B**) CGN70/20/10; (**C**) CGN60/20/20; (**D**) CGN50/20/30

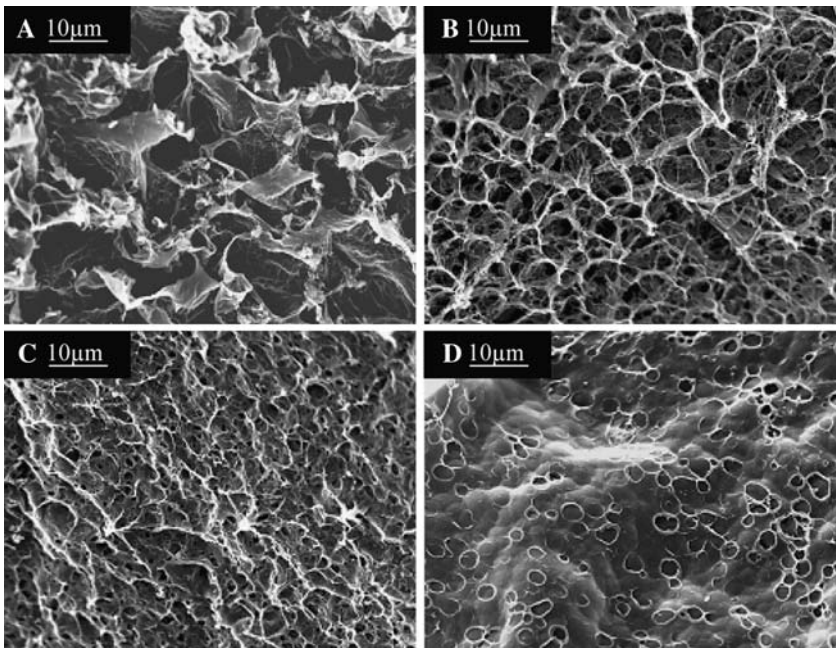

Fig. 11 Effect of PNIPAAm content on the surface morphology of chitosan/PEG/PNIPAAm hydrogel films swollen at 37 °C. PEG content retained at 20% by weight. (**A**) CGN75/20/5; (**B**) CGN70/20/10; (**C**) CGN60/20/20; (**D**) CGN50/20/30

PNIPAAm. As the PNIPAAm content increases, more crystalline domains were developed and intermolecular interaction became stronger. As a result, the water is hard to diffuse into the films and their swelling ratios reduced. In the newly formed crystalline domains, the molecules are closely packed, i.e., harder for water to penetrate or diffuse into. Hence, the swelling behaviors in crystalline and amorphous domains are different. As a result, the swollen films had a crumpled appearance because of their different swelling behavior in two different domains, and this difference became more prominent as their swelling ratio reduced. However, the pores of CGN50/20/30 may also be generated due to the delayed phase separation at a higher concentration of PNIPAAm component during the evaporation process [45].

When comparing to the data in Fig. 10 (at room temperature < LCST), the morphological data in Fig. 11 (37 °C) showed that more and larger pores were formed in blended films having PNIPAAm component at a temperature greater than the LCST of PNIPAAm. Normally, we

would expect smaller # and size of pores from these PNIPAAm-containing films at a temperature >LCST due to the thermo-induced shrinkage of PNIPAAm. The reason for the more and larger pores formed at 37 °C (>LCST) is believed to be attributed to differential swelling behavior between PNIPAAm and chitosan components within the blend. It is known that chitosan has no thermo-responsive property, so it would swell regardless of temperatures. When temperature reaches its LCST or higher, the PNIPAAm component in the blended films dehydrates and shrinks, thus the phase separation happens between PNIPAAm and its adjacent chitosan materials due to different swelling ratio. Because of the PNIPAAm shrinkage and phase separation, pores were formed in the blended films. The FT-IR spectra (see Figs. 2, 3) demonstrated that PNIPAAm remained in those freeze-dried films at both room temperature and 37 °C, which has been discussed in the FT-IR section. Therefore, the pores in the blends at 37 °C were formed mainly due to the thermo-induced shrinking of PNIPAAm.

At a higher temperature above the LCST of PNIPAAm, PNIPAAm moiety in the blended films becomes hydrophobic, which then makes the blended films hydrophobic, hence is difficult to take in water. The hydrophobicity, in turn, prevents the formation of pores due to the limited swelling. The hydrophobicity of the blended films increases with an increase in PNIPAAm content, which contributed to the reduction of pore size as shown from A (5% PNIPAAm) to D (30% PNIPAAm) in Fig. 11.

Mechanical property

The effect of PNIPAAm on the mechanical property of the chitosan/PNIPAAm films

The effect of the PNIPAAm content on the mechanical property of the chitosan/PNIPAAm films (no PEG component) is shown in Figs. 12 and 13. The data in these figures show that the stress, strain and toughness of the chitosan/PNIPAAm films deteriorated with the addition of PNIPAAm content, while the modulus was just slightly decreased first, then recovered. For example, the stress and strain were reduced 30% (from 60 MPa to 40 MPa) and 22% (from 27% to 5%), respectively, and the toughness reduced 80% (12.7–2.5 MPa) when the PNIPAAm content increased from 0% to 45%. Obviously, the chitosan/PNIPAAm films became less elastic due to the incorporation of PNIPAAm.

Films made from pure chitosan are very brittle [46]. With the incorporation of PNIPAAm, however, the chitosan/PNIPAAm films became even more brittle, which was evidenced by the drop of toughness (Fig. 13). It is known that toughness is inversely proportional to brittleness, so a decrease of toughness means an increase in brittleness. This brittleness could be attributed to the fact that, like chitosan, PNIPAAm is a rigid polymer (T_g 130 °C) [47], and its combination with chitosan makes the films even more brittle. The strain of the blended films decreased as the films became increasingly brittle. In addition, the X-ray data also shows that the incorporation of PNIPAAm into chitosan decreased the crystallinity of pure chitosan films (E in Fig. 4), which means the crosslinker density was reduced in the chitosan/PNIPAAm films, consequentially lower stress. Therefore, the mechanical property of the chitosan/PNIPAAm films was weakened.

Modulus is a measure of a material's ability to resist deformation upon a force. The higher the modulus, the less the film would deform upon a force. Figure 13 shows that the modulus decreased and then recovered with the addition of PNIPAAm, which might be attributed to the fact the both chitosan and PNIPAAm are both rigid polymers.

The effect of PEG on the mechanical property of the chitosan/PEG/PNIPAAm films

To improve the mechanical property of the chitosan/PNIPAAm films, PEG was introduced, and the PEG effect on the mechanical property of the blended chitosan/PEG/PNIPAAm films is shown in Figs. 14 and 15. In this series of blended films, the PNIPAAm content was kept at a constant (15%). The stress (Fig. 14) and modulus (Fig. 15) of the blended films decreased with an increase in PEG content, and most of the reduction in stress and modulus occurred upon an initial 5% and 10% incorporated PEG, respectively. For example, stress decreased 37% as PEG content increased from 0% to 30%, while the modulus decreased 47%. However, the strain and toughness of these blended films showed different behaviors; they increased first but decreased later after PEG content reached around 17%, showing that the chitosan/PEG/PNIPAAm blended films could attain the highest strain and toughness when PEG content was around 17%.

The chitosan/PEG/PNIPAAm films became more ductile and flexible after PEG was introduced at the amounts of 15–20% PEG composition (Figs. 14, 15). As a plasticizer, the inclusion of PEG disrupted the inter/intramolecular interactions between chitosan and PNIPAAm, thus the film could be elongated more easily under stress. This disruption factor, however, may be somewhat counter balanced by a higher level of crystallinity induced due to PEG incorporation. As discussed previously (X-ray diffraction data), more crystalline domains were formed with the introduction of PEG into chitosan/PNIPAAm film. The crystalline regions could act as physical crosslinkers to limit the elongation of the films as observed

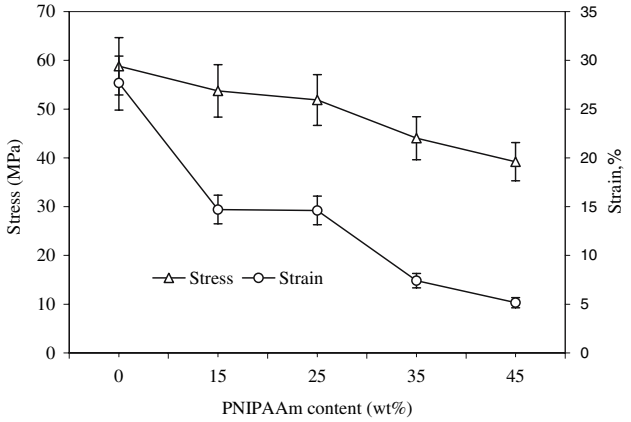

Fig. 12 Effect of PNIPAAm content on the tensile property of chitosan/PEG/PNIPAAm hydrogel films. PEG content retained at 0% by weight

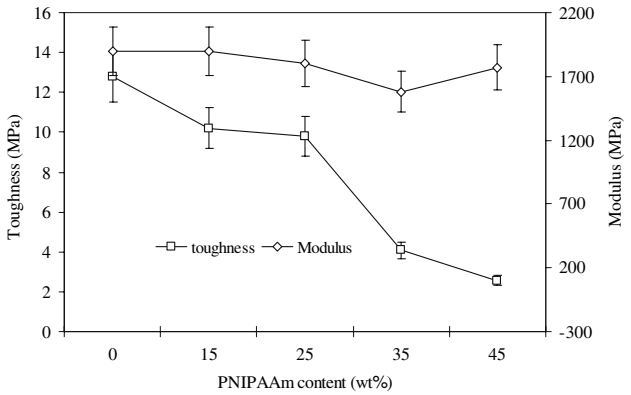

Fig. 13 Effect of PNIPAAm content on the toughness and modulus of chitosan/PEG/PNIPAAm hydrogel films. PEG content retained at 0% by weight

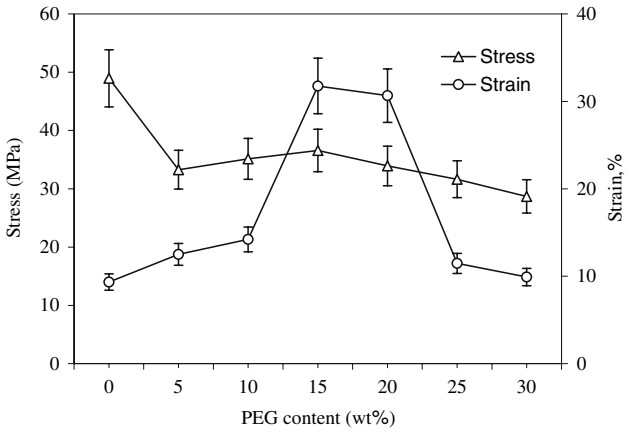

Fig. 14 Effect of PEG on the tensile property of chitosan/PNIPAAm/ PEG hydrogel films. PNIPAAm content retained at 15% by weight

(Fig. 14). A combination of plasticizer effect and physical crosslinking effect from induced crystalline domains as well as the dominance of either of these two effects could be responsible for the observed stress/strain (Fig. 14) and

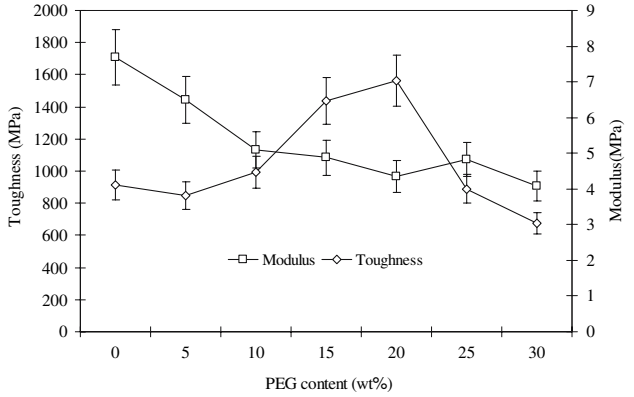

Fig. 15 Effect of PEG on the toughness and modulus of chitosan/ PNIPAAm/ PEG hydrogel films. PNIPAAm content retained at 15% by weight

toughness (Fig. 15) profiles as a function of PEG contents.

Fig. 14 shows that the effects of PEG incorporation into chitosan/PNIPAAm system on both stress and strain. The data indicated an initial weakened stress due to PEG incorporation followed by a slight increase in stress at around 15% of PEG content and a subsequent reduction in stress again thereafter. For the chitosan/PEG/PNIPAAm film, PNIPAAm could reduce stress by destroying the inter/ intra molecular interaction of chitosan macromolecules; while as a plasticizer, PEG further weakened such interactions. As discussed above, PEG may have a better intermolecular interaction with either chitosan or PNIPAAm at the concentration of 15–20%. So, the stress of the blended chitosan/PEG/PNIPAAm films was reduced with the addition of PEG, though there is a slight increase at around 15–20% PEG composition.

Figure 15 shows that the addition of 30% PEG into chitosan/PNIPAAm film led to a loss of 47% of its modulus. From the above discussion, we know that the addition of PEG weakens the interaction of chitosan macromolecule with each other and probably generates more free volume, by which they can deform easier under the same stress.

The effect of PEG content on mechanical property of chitosan was also reported before. Zhang et al. [30] reported that PEG alone could increase or decrease tensile strength of chitosan films at different PEG compositions. At a low PEG concentration (20%), the mechanical property could be improved, but at a high PEG concentration (33%), the mechanical property of the blended chitosan/ PEG film deteriorated. Budtova et al. [46] obtained a chitosan/PEO film with a better mechanical property (more ductile) at a 17% PEO composition than those made from pure chitosan. The best mechanical property was achieved at the stiochiometric composition between chitosan and PEO monomer units, in which they had the most intermolecular interaction.

The effect of PNIPAAm on the mechanical property of the chitosan/PEG/PNIPAAm films

Because the introduction of PEG into chitosan/PEG/PNIPAAm films could change their mechanical property, the PNIPAAm effect on the mechanical property of chitosan/PEG/PNIPAAm films at a constant 20% PEG content of the films was also investigated (Figs. 16, 17). Strain and toughness decreased as the PNIPAAm content increased; however, stress did not decrease until PNIPAAm reached 20%; while its modulus increased a little with the addition of PNIPAAm. For example, the stress reduced about 30% when PNIPAAm content increased from 0% to 30%; however, the strain and toughness reduced about 92% and 90%, respectively.

pH sensitivity

To investigate the pH effect on the swelling kinetics of the blended films, a series of different pH buffers (3.0, 4.0, 5.0, 7.0, and 10.0) were used. Figure 18 shows the results of the kinetics of swelling ratio of the CGN60/20/20 film at different pHs. The data clearly indicate that swelling ratios of these blended films were significantly influenced by pH. The CGN60/20/20 film could swell more and at a much faster rate in a lower pH medium than in a higher pH medium. For example, the film swelled to more than 60 times of its original weight at pH 3 in 240 min, while at pH 10, only 5 times. The distinctive swelling difference was attributed to the unique chemical structure of the chitosan component that has many pendant amino groups. In an acidic medium, the amino groups became protonated; the protonation of amino groups generated a higher proton concentration within the blended film than in its surrounding medium. This concentration gradient could give rise to osmotic pressure and resulted in a water flow into the hydrogel, a higher swelling. In addition, the electrostatic repulsion of the protonated $-NH^{+}_{3}$ groups along the chitosan polymer chain could also lead to an expansion of the network and hence a higher swelling. Therefore, the CGN60/20/20film can swell more and faster in a lower pH medium than in a higher pH medium.

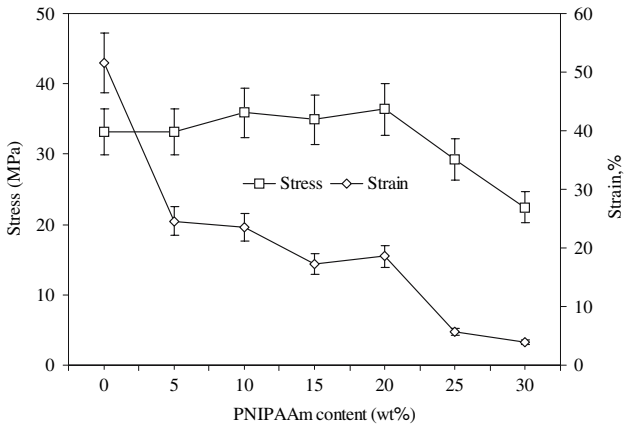

Fig. 16 Effect of PNIPAAm content on the tensile property of chitosan/PEG/PNIPAAm hydrogel films. PEG content retained at 20% by weight

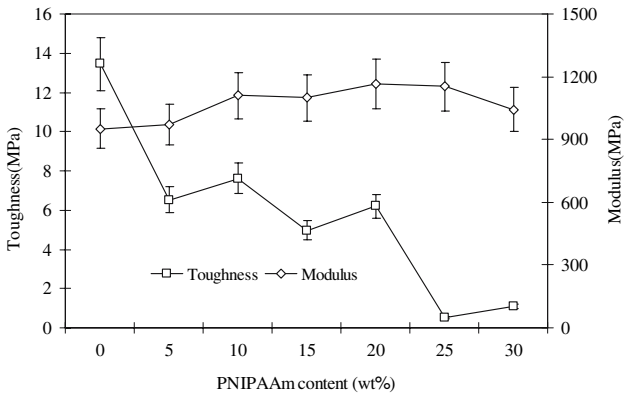

Fig. 17 Effect of PNIPAAm content on the toughness and modulus of chitosan/PEG/PNIPAAm hydrogel films. PEG content retained at 20% by weight

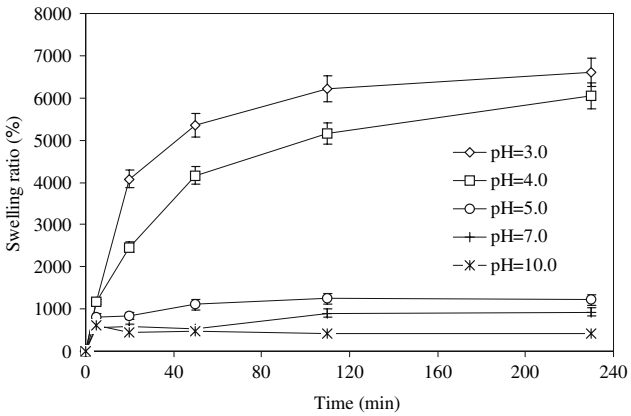

Fig. 18 Swelling kinetics of CGN60/20/20 hydrogel film at five different pHs

Conclusion

In this study, the chitosan-based films having both temperature and pH sensitivity were prepared by blending chitosan with PNIPAAm and PEG over a wide range of composition ratios. The thermal data revealed that the blended chitosan/PEG/PNIPAAm films had a LCST at around 32 °C due to PNIPAAm component in the films. The blended hydrogel films were also pH sensitive due to the amino groups of chitosan component in the films. The introduction of PEG into the chitosan/PNIPAAm system

changed its thermal, mechanical, swelling properties. The thermal data indicated that the chitosan/PNIPAAm films were apt to crystallize when PEG was added. The X-ray data further revealed that the incorporation of PEG into the chitosan/PNIPAAm system improved the level of crystallinity of the films. The crystalline domains acted as physical crosslinkers in the chitosan/PEG/PNIPAAm films and hence affected their swelling and mechanical properties. The blended films attained the highest strain when PEG component reached 17% in the films. SEM images showed significant morphological difference at temperatures below and above the LCST. At a temperature above the LCST, 3D porous structure of the chitosan/PEG/PNIPAAm films was found, and such unique SEM morphology was not observed at a temperature below the LCST (i.e., room temperature). It is believed that these pores were formed mainly due to the dehydration nature of PNIPAAm at temperatures above its LCST. The FT-IR data confirmed such a structure change was attributed to the existence of the PNIPAAm component in the films. Such temperature and pH sensitive hydrogel films may find some applications in the biomedical fields.

References

1. B. D. RATNER and A. S. HOFFMAN, ''ACS Symposium Series 31'' (Washington, DC: American Chemical Society, 1976), pp. 1–36
2. K. PARK and H. PARK, In ''*Concise Polymeric Materials Encyclopedia*,'' edited by J. C. Salamone (Boca Raton: CRC Press, 1999), pp. 1476–1478
3. A. S. HOFFMAN, *J. Control. Rel.* **6** (1987) 297
4. N. A. PEPPAS and J. KLIER, *J. Control. Rel.* **16** (1991) 203
5. G. H. CHEN and A. S. HOFFMAN, *Nature* **373** (1995)49
6. Z. S. LIU and P. CALVERT, *Adv. Mater.* **12** (2000) 288
7. S. J. KIM, S. G. YOON, Y. M. LEE and S. I. KIM, *Sensors Actuators B: Chem.* **88** (2003) 286
8. A. MANADA, T. TANAKA, D. KUNGWATCHAKUN and M. IRIE, *Macromolecules* **23** (1999) 1517
9. L.E. BROMBERG and E. S. RON, *Adv. Drug Deliver. Rev.* **31** (1998) 197
10. X. Z. ZHANG, Y. Y. YANG, T. S. CHUNG and K. X. MA, *Langmuir* **17** (2001) 6094
11. R. A. STILE, W. R. BURGHARDT and K. E. HEALY, *Macromolecules* **32** (1999) 7370
12. X. Z. ZHANG, Y. Y. YANG and T. S. CHUNG, *Langmuir* **18** (2002) 2538
13. M. KURISAWA, M. YOKOYAMA and T. OKANO, *J. Control. Rel.* **69** (2000) 127
14. S. K. LI and A. D'EMANUELE, *J. Control. Rel.* **75** (2001) 55
15. R. YOSHIDA, K. UCHIDA, Y. KANEKO, K. SAKAI, A. KIKUCHI, Y. SAKURAI and T. OKANO, *Nature* **374** (1995) 240
16. Y. QIO and K. PARK, *Adv. Drug Deliver. Rev.* **53** (2001) 321
17. H. ICHIKAWA and Y. FUKUMORI, *J. Control. Rel.* **63** (2000) 107
18. X. Z. ZHANG, R. X. ZHUO, J. Z. CUI and J. T. ZHANG, *Int. J. Pharm.* **235** (2002) 43
19. G. CHEN and A. C. HOFFMAN, *Nature* **373** (1995) 49
20. W. E. HENNINK and C. F. van NOSTRUM, *Adv. Drug Delver. Rev*. **54** (2002) 13
21. Y. IKADA, K. JAMSHIDI, H. TSUJI and S. H. HYON, *Macromolecules*, **20** (1987) 904
22. K. NAKAMAE, T. MIYATA and A. S. HOFFMAN, *J. Biomater. Sci. Polym. Ed.* **6** (1994) 79
23. T. INOUE, G. H. CHEN, A. S. HOFFMAN and K. NAKAMAE, *J. Bioact. Compat. Pol*. **13** (1998) 50
24. B. JEONG, S. W. KIM and Y. H. BAE, *Adv. Drug Delver. Rev.* **54** (2002) 37
25. K. KAMATH and K. PARK, *Adv. Drug Delver. Rev.* **11** (1993) 59
26. D. CAMPOCCIA, P. DOHERTY, M. RADICE, P. BURN, G. ABATANGELO and D. F. WILLIAMS, *Biomaterials* **19** (1998) 2101
27. G. D. PRESTWICH, D. M. MARECAK, J. F. MARECAK, K. P. VERCRUYSSE and M. R. ZIEBELL, *J. Control. Rel.* **53** (1998) 93
28. D. K. SINGH and A. R. RAY, *J. Macromol. Sci. R. M. C.C* **40** (2000) 69
29. V. DODANE and V. D. VILIVALAM, *Pharm. Sci. Technol. To.* **1** (1998) 246
30. M. ZHANG, X. H. LI, Y. D. DONG, N. M. ZHAO and X. F. ZHANG, *Biomaterials* **23** (2002) 2641
31. X. Z. ZHANG and C. C. CHU, *J. Appl. Polym. Sci.* **89** (2003) 1935
32. S. J. LEE, S. S. KIM and Y. M. LEE, *Carbohydr. Polym.* **41** (2000) 197
33. J. H. KIM and Y. M. LEE, *Polymer* **34** (1993) 1952
34. S. Y. KIM, S. M. CHO, Y. M. LEE and S. J. KIM, *J. Appl. Polym. Sci.* **78** (2000) 1381
35. G. W. URBANCZYK and B. LIPPSYMONOWICZ, *J. Appl. Polym. Sci.* **51** (1994) 2191
36. J. LI, J. F. REVOL and R. H. MARCHESSAULT, *J. Appl. Polym. Sci.* **65** (1997) 373
37. K. V. H. PRASHANTH, F. S. KITTUR and R. N. THARANATHAN, *Carbohydr. Polym.* **50** (2002) 27
38. F. L. MI, H. W. SUNG, S. S. SHYU, C. C. SU and C. K. PENG, *Polymer* **44** (2003) 6251
39. W. ZHAO, L. YU, X. ZHONG, Y. ZHANG and J. SUN, *J. Macromol. Sci. Phys.* **B34** (1995) 231
40. A. A. S. MACHADO, V. C. A. MARTINS and A. M. G. PLPIS, *J. Therm. Anal. Calorim*. **67** (2002) 491
41. S. Y. NAM and Y. M. LEE, *J. Membr. Sci.* **135** (1997) 161
42. J. S. AHN, H. K. CHOI and C. S. CHO, *Biomaterials* **22** (2001) 923
43. K. SAKURAI, T. MAEGAWA and T. TAKAHASHI, *Polymer* **41** (2000) 7051
44. A. K. BAJPAI and M. SHRIVASTAVA, *J. Biomater. Sci. Polym. Edu.* **13** (2002) 237
45. I. M. WIENK, R. M. BOOM, M. A. M. BEERLAGE, A. M. W. BULTE, C. A. SMOLDERS and H. STRATHMANN, *J. Membr. Sci.* **113** (1996) 361
46. T. BUDTOVA, N. BELNIKEVICH, L. KALYUZHNAYA, V. ALEXEEV, S. BRONNIKOV, S. VESNEBOLOTSKAYA and Z. ZOOLSHOEV, *J. Appl. Polym. Sci.* **84** (2002) 1114
47. M. T. GARAY, M. C. LLAMAS and E. IGLESIAS, *Polymer* **38** (1997) 5091